View metadata, citation and similar papers at core.ac.uk

brought to you by CORE

provided by CWI's Institutional Repository

Gelation in Porous Media, Part I: Constant Injection Rate

F.J. Vermolen, J. Bruining, C.J. van Duijn

Modelling, Analysis and Simulation (MAS)

MAS-R9928 September 30, 1999

Report MAS-R9928
ISSN 1386-3703

CWI
P.O. Box 94079
1090 GB Amsterdam
The Netherlands

CWI is the National Research Institute for Mathematics and Computer Science. CWI is part of the Stichting Mathematisch Centrum (SMC), the Dutch foundation for promotion of mathematics and computer science and their applications.
SMC is sponsored by the Netherlands Organization for Scientific Research (NWO). CWI is a member of ERCIM, the European Research Consortium for Informatics and Mathematics.

Copyright © Stichting Mathematisch Centrum
P.O. Box 94079, 1090 GB Amsterdam (NL)
Kruislaan 413, 1098 SJ Amsterdam (NL)
Telephone +31 20 592 9333
Telefax +31 20 592 4199

Gel Placement in Porous Media
Part I: Constant Injection Rate

F.J. Vermolen
CWI
P.O.Box 94079, 1090 GB Amsterdam, The Netherlands

J. Bruining
Faculty of Applied Earth Sciences
Delft University of Technology
Mijnbouwstraat 120, 2628 RX Delft, The Netherlands

C.J. van Duijn
CWI
P.O. Box 94079, 1090 GB Amsterdam, The Netherlands

ABSTRACT

In this paper we analyse advective transport of polymers, crosslinkers and gel, taking into account non-equilibrium gelation, gel adsorption and crosslinker precipitation. In absence of diffusion/dispersion the resulting model consists of hyperbolic transport-reaction equations. These equations are studied in several steps using mainly analytical techniques. For simple cases, we obtain explicit travelling wave solutions, whereas for more complicated cases we rely on analytical techniques to analyse the problem qualitatively. Finally, a numerical solution for the full system of equations is obtained. The results developed in this study can be used to validate numerical solutions obtained from commercial simulators.

1991 Mathematics Subject Classification: 35R35, 76S05
Keywords and Phrases: hyperbolic equations, travelling wave, gelation, adsorption, porous media
Note: Research funded by the European Union (Welgel project).

1. Introduction

Mature oil fields (oil fields are often referred to as reservoirs) suffer from excessive water production. Large water production creates serious environmental problems concerning water waste disposal. Additionally the operating cost increase and large oil reserves remain unproduced. A major cause for high water production is water-chanelling through high permeability layers in reservoirs.

To minimise water production, polymers and crosslinkers in aqueous solution are injected, aiming at decreasing the permeability of well-permeable layers. Polymers react with crosslinkers and then form gel (gelation). The gels used are hydrophilic, i.e. they easily

dissolve in water and hardly in oil. Consequently, the water viscosity increases thereby reducing water mobility, whereas the oil viscosity and mobility remain practically unchanged. The gel is adsorbed on the skeleton of the reservoir (gel placement). As a consequence:

- webbs may arise from bridging adsorption [8],
- the flow area of the pore may decrease due to layer formation on the skeleton of the porous medium.

Both processes cause a decrease of the permeability. Since water flows near the skeleton of the porous medium, the first process effects mainly the relative permeability of water. Zitha et al [9] calculated changes of the relative permeabilities of oil and water through a gel treated porous medium. The difference found was significant.

Crosslinker precipitation depends crucially on the acidity of the fluid. High acidity results in high crosslinker solubility which in turn prevents precipitation. When the degree of acidity decreases, the crosslinker solubility decreases as well and precipitation will take place. This was shown by Stavland et al [5]. Under practical circumstances one uses an acetatic preflush to increase the acidity and hence to reduce the crosslinker precipitation.

Stavland et al [5] give a detailed description of the chemical processes that occur during gel placement in porous media. In this paper we investigate the consequences of these processes when transport takes place. For this purpose we formulate a transport-reaction model taking into account:

1. constant injection rate,
2. convection of polymers, crosslinkers and gel,
3. gelation reaction, i.e. polymer + crosslinker $\leftrightarrow$ gel,
4. crosslinker precipitation,
5. gel-adsorption of the gel in the reservoir.

The assumption of constant injection rate, when combined with fluid incompressibility and simple flow geometries, implies a given stationary discharge field. Hence we do not take into account the influence of gel placement on the fluid flow. This will be treated in Part 2 of this work where we consider constant pressure boundary conditions in a heterogeneous reservoir. Note that we disregard effects of diffusion and dispersion in this model, since the porous medium is assumed to be homogeneous and isotropic.

The aim of the paper is to understand the effect of the various chemical processes during gel placement in porous media. We do this by employing mainly analytical methods. Depending on the degree of complexity we present explicit solutions, qualitative statements about the behaviour of solutions and finally a numerical solution technique.

In Section 2 we formulate a model for gel placement in porous media. We give explicit solutions and qualitative statements about solutions in Section 3. Conclusions are summarised in Section 4.

2. Model Formulation

In this section we formulate a model for gel placement in porous media and we treat the transport, chemical processes and model equations in separate subsections. We consider a radially symmetric reservoir of constant thickness, H (m), and of infinite horizontal extend. At the central axis a well with radius r_w (m) is present which extends over the full thickness of the reservoir. Water containing polymers and crosslinkers at constant concentrations $\hat{c}_p$ (mol/m^3) and $\hat{c}_x$ (mol/m^3), respectively, is injected through the well into the reservoir at a constant rate Q_{in} (m^3/s). Initially polymers, crosslinkers and gels are absent in the reservoir.

2.1 Transport

Let the porous medium be homogeneous and isotropic with porosity ϕ. Further, let the fluid be incompressible. Assuming the flow to be uniformly distributed across the thickness of the reservoir, the specific discharge (radial component) is given by:

$$q = q(r) = \frac{Q_{in}}{2\pi H r}, \quad r > r_w, \tag{2.1}$$

where r (m) denotes the distance towards the central axis of the reservoir.

2.2 Chemical Processes

First we consider the gelation process:

$$K(P)_{aq} + L(X)_{aq} \leftrightarrow (G)_{aq},$$

Here the subscript $()_{aq}$ denotes that P, X and G are in aqueous solution and P, X and G denote polymers, crosslinkers and gel respectively. Their concentrations c_p, c_x and c_g respectively are expressed in mol/m^3. Further K and L are the stoichiometric parameters of the gelation reaction. Following Stavland et al [5] we disregard gel-decay with respect to gelation. This assumption implies that gelation continues until either crosslinkers or polymers are consumed. The gelation rate, $J\,(mol/m^3 s)$, is given by:

$$J = J(c_p, c_x) = a \cdot {c_p}^k {c_x}^l, \tag{2.2}$$

where a $(\left[\frac{m^3}{mole}\right]^{k+l+1} \frac{1}{s})$ denotes the gelation rate constant. The exponents k, l do not necessarily have to be equal to K and L.

Next we consider crosslinker precipitation. Crosslinkers (X) can react with OH-ions according to the following reaction:

$$(X)_{aq} + \mu(OH)_{aq} \leftrightarrow X(OH)_{\mu}\,(s).$$

Here (s) indicates that the reaction product is a solid. Let A_x be the precipitated crosslinker concentration (mol/m^3). According to Stavland et al [5] the reaction rate in presence of precipitated crosslinkers is given by

$$\frac{\partial A_x}{\partial t} = k_1 \left((c_x c_{OH}^{\mu})^{\beta} - k_2 \right).$$

Here $\beta > 1$ is a precipitation parameter introduced by Stavland et al [5]. Further k_1 $(\left[\frac{mole}{m^3}\right]^{1-\beta(\mu+1)} \frac{1}{s})$ and k_2 $(\left[\frac{mole}{m^3}\right]^{\beta(\mu+1)})$ are reaction rate constants. Suppose that initially $A_x = 0$ and $(c_x c_{OH}^{\mu})^{\beta} < k_2$ then above equation gives a $\frac{\partial A_x}{\partial t}$ with a negative sign and hence A_x becomes negative as well. Therefore we extend above equation with the results of Knabner & Van Duijn [3] to obtain

$$\frac{\partial A_x}{\partial t} = k_1 \cdot (c_x (c_{OH})^{\mu})^{\beta} - k_2 \cdot w), \tag{2.3}$$

where the function w is introduced by Knabner & van Duijn [3] to quarantee that A_x remains nonnegative at all stages. This function satisfies $w \in H(A_x)$ with:

$$H(s) = \begin{cases} 0, & s < 0 \\ \in [0,1], & s = 0 \\ 1, & s > 0 \end{cases}$$

In Section 3 we show that this formulation describes precipitation and dissolution properly. Then we will see that $w = r$ as $A_x = 0$ and $r < 1$. Equation (2.3) can be rearranged, with $K_{sol} := (\frac{k_2}{k_1})^{\frac{1}{\beta}}$, into:

$$\frac{\partial A_x}{\partial t} = k_2 \cdot \left(\left(\frac{c_x c_{OH}^{\mu}}{K_{sol}} \right)^{\beta} - w \right) =: k_p \left(r(c_x, c_{OH}) - w \right). \tag{2.4}$$

The constant K_{sol} is the solubility product. In Section 3 we will show that crosslinker precipitation occurs if and only if:

$$c_x \cdot c_{OH}^{\mu} > K_{sol}. \tag{2.5}$$

Finally we consider gel adsorption. Let $A(r,t)$ denote the concentration of adsorbed gel, expressed in $mole/kg$ porous medium. The non-equilibrium adsorption rate is modelled by:

$$\frac{\partial A}{\partial t} = k_a \cdot (\phi(c_g) - A). \tag{2.6}$$

where k_a $(1/s)$ is the gel adsorption rate constant and $\phi(c_g)$ (mol/kg) the gel adsorption isotherm.

2.3 Model Equations and scaling

Here we formulate the mass balance equations for the chemical species. Since the concentrations at the well are constant over the height of the reservoir and gravity can be disregarded, all concentrations are functions of the horizontal distance r and time t only. Consequently, we have for $r > r_w$ and $t > 0$, the mass-balance equations:

- Polymers, subject to convection and gelation:

$$\phi \frac{\partial c_p}{\partial t} + \frac{\tilde{q}}{r}\frac{\partial c_p}{\partial r} = -\phi K J(c_p, c_p), \tag{2.7}$$

  where $\tilde{q} = \frac{Q}{2\pi H}$.

- Crosslinkers, subject to convection, gelation and precipitation:

$$\phi \frac{\partial c_x}{\partial t} + \frac{\tilde{q}}{r}\frac{\partial c_x}{\partial r} = -\phi \left(L J(c_p, c_x) + \frac{\partial A_x}{\partial t} \right). \tag{2.8}$$

- Gel, subject to convection, gelation and gel adsorption:

$$\phi \frac{\partial c_g}{\partial t} + \frac{\tilde{q}}{r}\frac{\partial c_g}{\partial r} = \phi M J(c_p, c_x) - \rho_s (1-\phi)\frac{\partial A}{\partial t}. \tag{2.9}$$

- OH-ions, subject to convection and precipitation:

$$\phi \frac{\partial c_{OH}}{\partial t} + \frac{\tilde{q}}{r}\frac{\partial c_{OH}}{\partial r} = -\mu\phi \frac{\partial A_x}{\partial t}. \tag{2.10}$$

Here, the crosslinker precipitation rate ($\frac{\partial A_x}{\partial t}$), gel adsorption rate ($\frac{\partial A}{\partial t}$) and gelation rate ($J$) are given by equations (2.4), (2.6) and (2.2), respectively.

Introducing the transformation $x = \frac{Q\phi}{4\pi H}(r^2 - r_w^2)$ and redefining $A := \rho_s \frac{1-\phi}{\phi} A$ and $\phi(c_g) := \rho_s \frac{1-\phi}{\phi}\phi(c_g)$, we arrive at the set of equations (with $w \in H(A_x)$):

$$(P1) \begin{cases} \dfrac{\partial c_p}{\partial t} + \dfrac{\partial c_p}{\partial x} = -K \cdot J(c_p, c_x) \\ \dfrac{\partial (c_x + A_x)}{\partial t} + \dfrac{\partial c_x}{\partial x} = -L \cdot J(c_p, c_x) \\ \dfrac{\partial (c_g + A)}{\partial t} + \dfrac{\partial c_g}{\partial x} = J(c_p, c_x) \\ \dfrac{\partial (c_{OH} + \mu A_x)}{\partial t} + \dfrac{\partial c_{OH}}{\partial x} = 0 \\ \dfrac{\partial A}{\partial t} = k_a \cdot (\phi(c_g) - A) \\ \dfrac{\partial A_x}{\partial t} = k_p \cdot (r(c_x, c_{OH}) - w) \end{cases}$$

which we need to solve, subject to the initial condition for $x > 0$

$$(IC)\begin{cases} c_p(x,0) = 0, \quad c_x(x,0) = 0, \quad c_g(x,0) = 0, \\ \\ c_{OH}(x,0) = c^0_{OH}, \quad A(x,0) = 0, \quad A_x(x,0) = 0, \end{cases}$$

and boundary condition for $t > 0$

$$(BC)\begin{cases} c_p(0,t) = \hat{c}_p, \quad c_x(0,t) = \hat{c}_x, \\ \\ c_g(0,t) = 0, \quad c_{OH}(0,t) = \hat{c}_{OH}. \end{cases}$$

3. Analysis of the model

As a first observation we note that the equations for the (precipitated) crosslinkers, polymers and OH-ions are independent of the (adsorbed) gel concentration. Therefore we can treat these equations separately.

First we consider crosslinker precipitation from equation (2.4). Subsequently we analyse the profiles of (precipitated) crosslinkers, polymers and OH-ions. Finally we treat several stages of gel-adsorption.

3.1 Crosslinker precipitation

In this section we show that equation (2.4), and in particular the introduction of the function w, describes all properties of the precipitation-dissolution process away from possible shock curves in the x,t-plane. For convenience we write $r = r(c_x, c_{OH})$ in equation (2.4) and we drop the space dependence in A_x. We show first that $A_x(0) \geq 0$ implies $A_x(t) \geq 0$ for all $t > 0$. Arguing by contradiction, suppose $A_x(\overline{t}) < 0$ for some $\overline{t} > 0$. Since A_x continuously depends on t, then exists $0 \leq \underline{t} < \overline{t}$ such that $A_x(t) < 0$ for all $\underline{t} < t \leq \overline{t}$ and $A_x(\underline{t}) = 0$. Next we multiply (2.4) by A_x and integrate the result over the interval $(\underline{t}, \overline{t})$. This gives

$$0 \leq \frac{A_x^2(\overline{t})}{2} = k_p \int_{\underline{t}}^{\overline{t}} (r - w) A_x dt. \tag{3.1}$$

Since $r \geq 0$ and $w = 0$ on $(\underline{t}, \overline{t})$, we see that the right hand side of (3.1) is non-positive, giving the contradiction. Clearly $r > 1$ implies precipitation ($\frac{\partial A_x}{\partial t} > 0$) since $w \leq 1$. Conversely, dissolution, i.e. $A_x > 0$ and $\frac{\partial A_x}{\partial t} < 0$, implies $r < 1$. This follows directly from the requirement that $w = 1$ where $A_x > 0$. Finally, if $A_x = 0$ in some interval, then $\frac{\partial A_x}{\partial t} = 0$ as well, leading to $w = r$.

In the construction of the solutions presented in Section 3.2. we use the following observation: if $A_x(t^*) = 0$ for some $t^* \geq 0$ and $r < 1$ for $t > t^*$, then $A_x(t) = 0$, with $w = r$ as a consequence, for all $t > t^*$. This follows directly from identity (2.3).

3.2 The crosslinker, polymer and OH profiles
In this section we consider the crosslinker, polymer and OH equations, which can be solved without apriori knowledge of the (adsorbed) gel concentration. Combining these equations we observe that

$$v := \mu(c_x - \frac{L}{K}c_p) - c_{OH}, \tag{3.2}$$

satisfies

$$\frac{\partial v}{\partial t} + \frac{\partial v}{\partial x} = 0.$$

Thus v is in this respect a conserved quantity, only subject to convection and can be expressed by

$$v(x,t) = (v^0 - \hat{v})H(x-t) + \hat{v},$$

where $\hat{v} := \mu(\hat{c}_x - \frac{L}{K}\hat{c}_p) - \hat{c}_{OH}$ and $v^0 := \mu(c_x^0 - \frac{L}{K}c_p^0) - c_{OH}^0$. We can interprete v as a scaled (positive) electric charge of the solution.

Using v, we eliminate c_{OH} from the equations for c_p and c_x. This leaves us with the system, for $x > 0$ and $t > 0$:

$$(P1a) \begin{cases} \dfrac{\partial c_p}{\partial t} + \dfrac{\partial c_p}{\partial x} = -KJ(c_p, c_x) \\ \dfrac{\partial c_x}{\partial t} + \dfrac{\partial c_x}{\partial x} = -LJ(c_p, c_x) - k_p(\tilde{r}(c_x, c_p, v) - w) \end{cases}$$

where $\tilde{r}(c_x, c_p, v) := r(c_x, \mu(c_x - \frac{L}{K}c_p) - v)$.
We consider the following two cases:

i) $\hat{r} := \tilde{r}(\hat{c}_x, \hat{c}_p, \hat{v}) \leq 1$. Due to the gelation reaction we have $\tilde{r} < 1$ and consequently $A_x = 0$, $w = \tilde{r}$ for all $x, t > 0$. Hence, equations (P1a) reduce to

$$\begin{cases} \dfrac{\partial c_p}{\partial t} + \dfrac{\partial c_p}{\partial x} = -KJ(c_p, c_x) \\ \dfrac{\partial c_x}{\partial t} + \dfrac{\partial c_x}{\partial x} = -LJ(c_p, c_x) \end{cases}$$

We seek solutions of the form:

$$c_p, c_x(x,t) = \overline{c}_p, \overline{c}_x(x) \cdot H(t-x). \tag{3.3}$$

This leads to system

$$\begin{cases} \dfrac{d\overline{c}_p}{dx} = -KJ(\overline{c}_p, \overline{c}_x), \\ \dfrac{d\overline{c}_x}{dx} = -LJ(\overline{c}_p, \overline{c}_x), \end{cases}$$

for $x > 0$ subject to $\tilde{c}_p(0) = \hat{c}_p$ and $\tilde{c}_x(0) = \hat{c}_x$. Clearly $\overline{c}_p = \frac{K}{L}(\overline{c}_x - \hat{c}_x) + \hat{c}_p$. We distinguish the cases:

1. $\hat{c}_p < \frac{K}{L}\hat{c}_x$. Then $\overline{c}_p(x) \to 0$, $\overline{c}_x(x) \to \hat{c}_x - \frac{L}{K}\hat{c}_p$ as $x \to \infty$. In other words, all polymers will be consumed, leaving a positive crosslinker concentration. As in [6] the following can be established. If $k \geq 1$ (see equation 2.2) then $\overline{c}_p > 0$, $\overline{c}_x > \hat{c}_x - \frac{L}{K}\hat{c}_p$ for all $x > 0$. However, if $k < 1$, then there exists a distance $x_D > 0$ such that

$$\overline{c}_p(x) > 0,\ \overline{c}_x(x) > \hat{c}_x - \tfrac{L}{K}\overline{c}_p \text{ for } 0 < x < x_D$$

$$\overline{c}_p(x) = 0,\ \overline{c}_x(x) = \hat{c}_x - \tfrac{L}{K}\overline{c}_p \text{ for } x \geq x_D$$

   The distance x_D is given by

$$x_D = \frac{1}{K}\int_0^{\overline{c}_p} \frac{1}{J(s, \hat{c}_x + \frac{L}{K}(s - \hat{c}_p))} ds.$$

2. $\hat{c}_p > \frac{K}{L}\hat{c}_x$. Then $\overline{c}_p(x) \to \hat{c}_p - \frac{K}{L}\hat{c}_x$, $\overline{c}_x(x) \to 0$ as $x \to \infty$, indicating that now all crosslinkers will be consumed, leaving a positive polymer concentration. As above the limit values can be attained at finite or infinite distance, depending whether $k < 1$ or $l < 1$.

An example of crosslinker concentration profiles is shown in Figure 1. Input values are taken from Table 1.

Parameter values	
a	1
K	1
L	5
k	0.5
l	2.5
$\hat{c}_x$	2
$\hat{c}_p$	0.2

Table 1

ii) $\hat{r} > 1$. This case implies precipitation. Due to gelation and precipitation $\tilde{r}(c_x, c_p, v) < \hat{r}$ in the entire x, t-plane. To construct a solution of equations (P1a) and (IC) we distinguish the following subdomains in the x, t-plane, see Figure 2.

$$\begin{cases} I := \{(x,t) : t > 0, x > t\}, \\ II := \{(x,t) : t > 0, 0 < x < \min(x_1, t)\}, \\ III := \{(x,t) : t > x, x_1 < x < t\}, \end{cases}$$

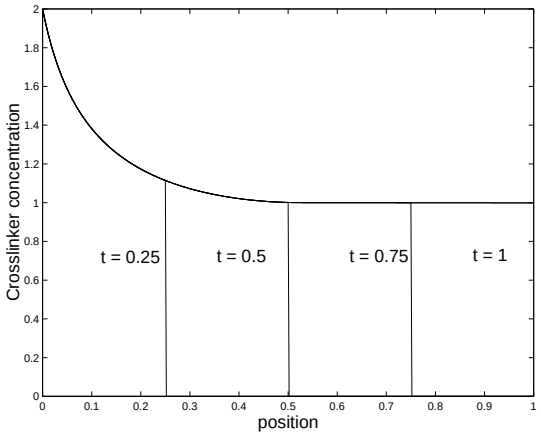

Figure 1: Crosslinker concentration profiles at the times: $t = 0.25,\ 0.5,\ 0.75,\ 1$.

where $x_1 > 0$ will be defined later.

The hyperbolic nature of (P1a) implies that

$$c_p = c_x = A_x = 0,\ v = v_0 \ (\text{ or } c_{OH} = c_{OH}^0) \text{ in } I.$$

Since $v = \hat{v}$ along characteristics $t = x + t_0$, with $t_0 > 0$, and the boundary conditions are constant, integration of equations (P1a) along these characteristics yields a smooth solution which depends on x only in the remaining region $0 < x < t$, $t > 0$.

Since $\tilde{r} > 1$ and c_p, c_x decrease along characteristics, we arrive at the situation sketched in Figure 2: i.e. $\tilde{r} > 1$, with $w = 1$ and $A_x > 0$ in region II and $\tilde{r} < 1$, with $w = r$ and $A_x = 0$ in III. The monotonicity of the concentrations uniquely defines the position x_1 where $\tilde{r} = 1$. Hence along characteristics $x = t + t_0$ with $t_0 > 0$ we have to solve the system

$$(P1b) \quad \begin{cases} \dfrac{dc_x}{dx} = -LJ(c_p, c_x) - k_p(\tilde{r}(c_x, c_p, \hat{v}) - w) \\ \\ \dfrac{dc_p}{dx} = -KJ(c_p, c_x) \end{cases}$$

for $x > 0$ where

$$w = \begin{cases} 1, & x < x_1, \\ \\ \tilde{r}(c_p, c_x, \hat{v}), & x > x_1. \end{cases}$$

Explicit solutions to the system (P1b) can only be constructed for a limited class of functions J and $\tilde{r}$. In general one has to rely on phase plane methods to gain insight in the behaviour of its solutions. The underlying idea is to consider solutions of (P1b) as orbits in the c_x, c_p phase plane. The behaviour of such orbits crucially depends on the value of $\tilde{r}$: i.e. whether or not precipitation occurs. Combining the expressions for $\tilde{r}$ and $v = \tilde{v}$, we

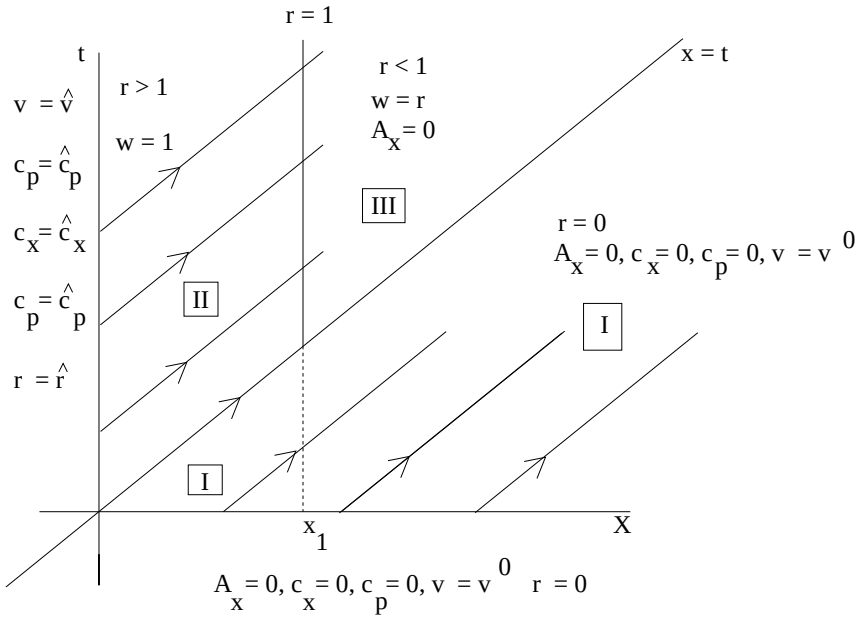

Figure 2: Characteristics in the x,t plane.

find at a trajectory that

$$\tilde{r} \gtrless 1 \text{ if and only if } c_p \lessgtr f(c_x; \hat{v}), \tag{3.4}$$

where

$$f(c_x; \hat{v}) = \frac{K}{L\mu}\left(\mu c_x - \hat{v} - (\frac{K_{sol}}{c_x})^{1/\mu}\right). \tag{3.5}$$

Note that the boundary conditions $\hat{c}_x$, $\hat{c}_p$ and $\hat{c}_{OH}$ uniquely determine $\hat{v}$ through (3.2) and thereby the location of the curve $c_p = f(c_x; \hat{v}$ in the c_x, c_p plane. Two typical cases are shown by the dashed curves in Figure 3. Input values are taken from Table 2.

Parameter	*values*
a	1
K	1
L	5
k	0.5
l	2.5
$\hat{c}_x$	2
$\hat{c}_p$	0.2
$\hat{c}_{OH}$	1
c^0_{OH}	1
μ	1
k_p	1
K_{sol}	0.2

Table 2

The asymptotes of $c_p = f(c_x; \hat{v})$, are given by

$$c_p = \frac{K}{L} c_x - \frac{K}{L\mu} \hat{v}. \tag{3.6}$$

Comparing with (3.2), this implies that the boundary condition $\hat{c}_x$ and $\hat{c}_p$, i.e. the starting positions of orbits in the c_x, c_p plane, are always below (for $\hat{c}_{OH} > 0$) or at (for $c_{OH} = 0$) the asymptotes.

Starting with boundary conditions above dashed curve (1), gives $\tilde{r} < 1$, $w = \tilde{r}$ (no precipitation takes place) and from (P1b)

$$\frac{dc_p}{dc_x} = \frac{K}{L}, \tag{3.7}$$

i.e. solution orbits are parallel to the asymptote of (3.4,3.5). When boundary conditions are taken below curve (3.4,3.5), $\tilde{r} > 1$ and $w = 1$ as long as the solution orbit is below this curve. Then the orbit satisfies

$$\frac{dc_p}{dc_x} = \frac{K}{L + k_p \frac{\tilde{r}-1}{J(c_p, c_x)}} < \frac{K}{L}, \tag{3.8}$$

and the intersection with curve (3.4,3.5) determines the position x_1 when the precipitation stops. For $x > x_1$, the orbit satisfies again (3.7) and then continues parallel to the asymptote of (3.4,3.5). These two possibilities are shown by the orbits (1) and (2) in Figure 3. Note that these orbits correspond to different values of c_{OH}: orbit (1) results from the smaller $\hat{c}_{OH}$. To obtain the concentration profiles requires a second integration. Figure 4 gives the resulting c_{OH} profile at different times. Note that these profiles show a minimum in c_{OH} concentration ($\hat{c}_{OH} = c^0_{OH} = 1$) caused by precipitation. As in case i) we can select boundary conditions such that either all polymers or all crosslinkers will be consumed, at

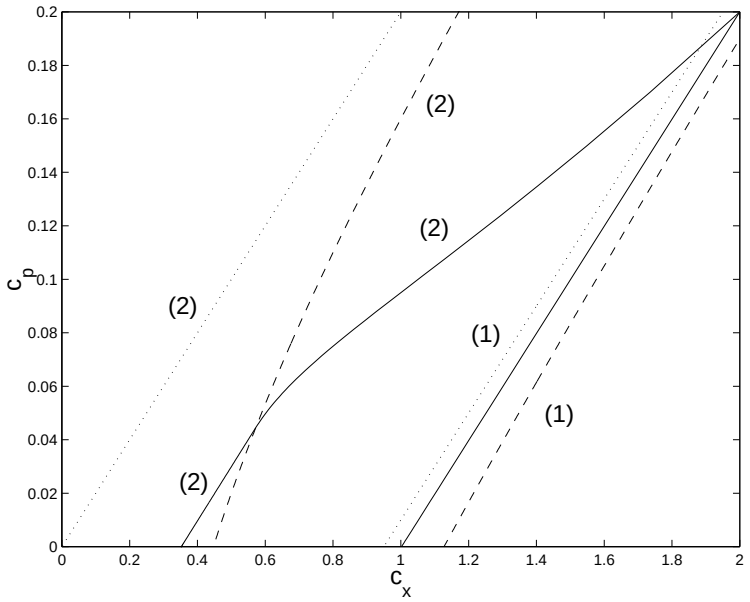

Figure 3: Two orbits in the c_x, c_p phase plane. The input parameters are equal except for the value of $\hat{c}_{OH}$: situation (1) corresponds to the lower $\hat{c}_{OH} = 0$ and situation (2) corresponds to $\hat{c}_{OH} = 1$. The dashed lines indicate the curves $c_p = f(c_x; \hat{v})$ for each set of boundary conditions. At the intersection of the solid and dashed lines we have $\tilde{r} = 1$. The dotted lines represent asymptotes of the curve $c_p = f(c_x; \hat{v})$.

finite or infinite distance. The same criteria apply.

In Figure 5 we investigate the influence of the solubility product K_{sol}. Decreasing K_{sol}, implies that the curve $\tilde{r} = 1$ moves upwards in the phase plane, ending on the asymptote (3.6) when $K_{sol} = 0$. As a consequence the orbits (or concentrations) are subject to precipitation over an increasing distance in the c_x, c_p phase plane. This is shown in Figure 5, where the orbits emerge from the same boundary conditions. The corresponding precipitated crosslinker concentration A_x, taken at the same time $t = 0.5$, is shown in Figure 6.

3.3 The gel profile

From the previous subsection it appears that

$$c_p,\ c_x(x,t) = \overline{c}_p,\ \overline{c}_x(x) \cdot H(t-x).$$

This implies that $J(c_p, c_x)$ can be written as

$$J(c_p, c_x) = J(x) \cdot H(t-x).$$

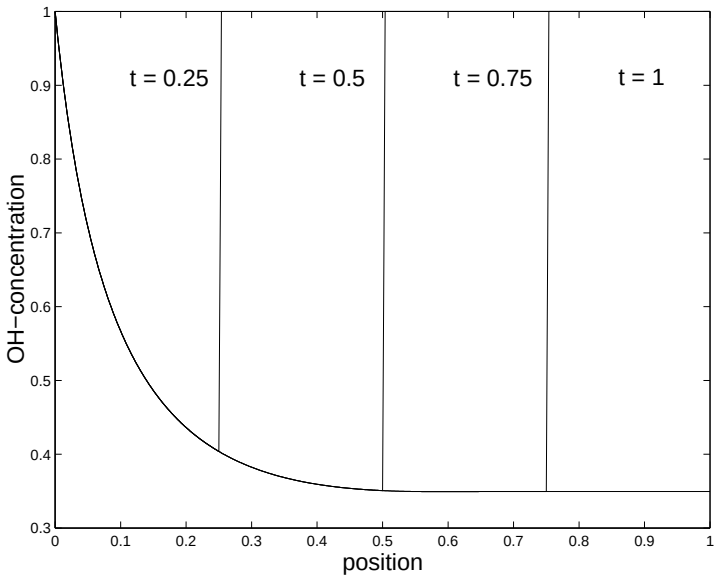

Figure 4: OH-concentration profiles at several times. Input data are taken from Table 2.

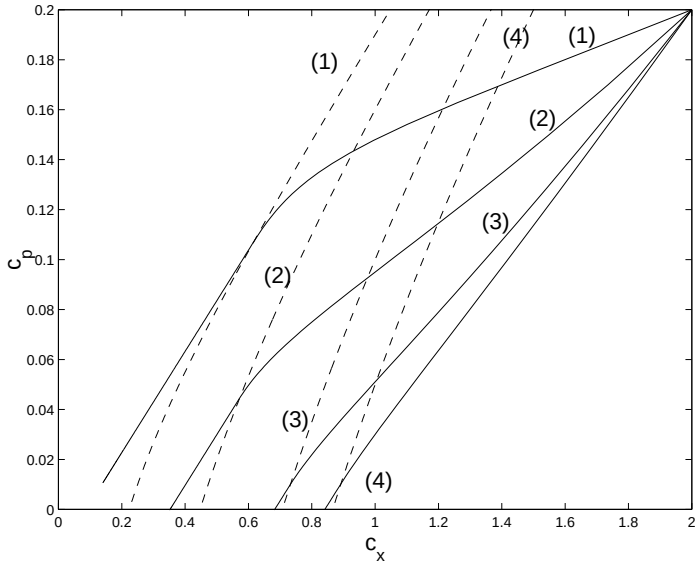

Figure 5: Some computed orbits in the phase plane for different values of K_{sol}. Situations (1-4) correspond to respectively $K_{sol} = 0.05, 0.2, 0.5$ and 0.75.

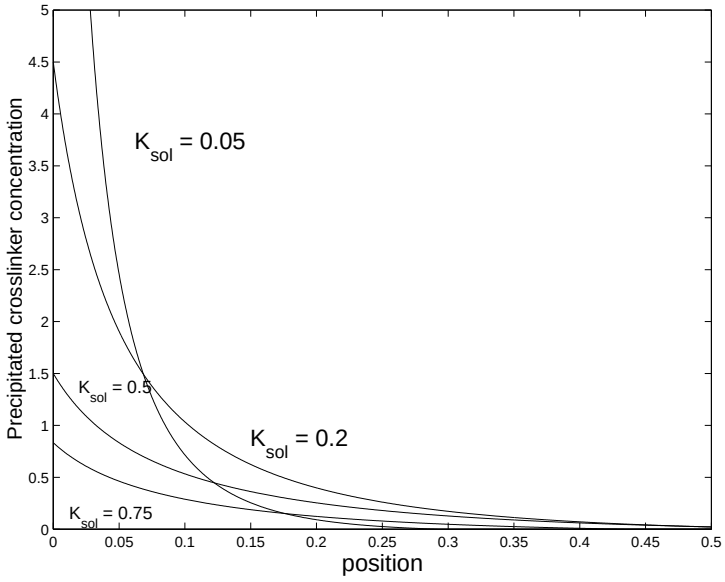

Figure 6: Some computed orbits in the phase plane for different values of K_{sol}.

We shall restrict ourselves to the case when $J(x) = 0$ for $x \geq x_D$: meaning that either polymers or crosslinkers are consumed for $x \geq x_D$. Hence the source term is known in the gel equations. For $x > 0$ and $t > 0$ they read as

$$(P2) \quad \begin{cases} \dfrac{\partial c_g}{\partial t} + \dfrac{\partial A}{\partial t} + \dfrac{\partial c_g}{\partial x} = J(x)\, H(t-x), \\ \\ \dfrac{\partial A}{\partial t} = k_a(\phi(c_g) - A), \end{cases}$$

where c_g and A satisfy initial and boundary conditions (IC), (BC), i.e.

$$c_g(0,t) = 0 \qquad \text{for all } t > 0,$$

$$c_g(x,0) = 0 = A(x,0) \qquad \text{for all } x > 0.$$

In general we are not able to construct (semi) explicit solutions. Only when simplified assumptions are made, some qualitative remarks can be made. Otherwise we have to rely on numerical techniques.

To solve (P1) and (P2) we use a finite volume method, see for instance [4], [1]. To avoid numerical dispersion as much as possible, we apply the Van Leer limiter [7], see also Hundsdorfer [2] for a well presented survey. The time integration is done with an explicit trapezium rule as in Hundsdorfer [2].

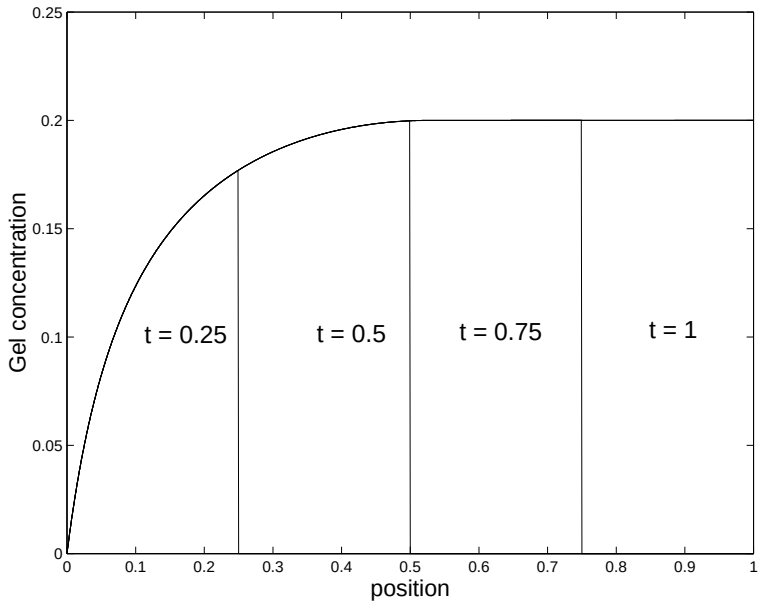

Figure 7: Gel concentration profiles with $k_a = 0$ at times: $t = 0.25$, 0.5, 0.75 and 1. Input data are taken from Table 1. Note that here $x_D = 0.52$.

Next we discuss some simplifications concerning (P2). If we assume that no adsorption takes place, i.e. $k_a = 0$ in (P2), then $A = 0$ and as before:

$$c_g(x,t) = \overline{c}_g(x) \cdot H(t-x).$$

The function $\overline{c}_g(x)$ is then given by the integral over the known source function $J(x)$:

$$\overline{c}_g(x) = \int_0^x J(s)ds, \quad \text{with} \quad c_g^* := \overline{c}_g(x_D) \quad \text{being its maximal value.}$$

The corresponding solution is shown in Figure 7.

If the adsorption is instantaneous, i.e. $k_a = \infty$, then (P2) reduces to the single equation (see [6] for a theoretical justification)

$$\frac{\partial}{\partial t}\left\{c_g + \phi(c_g)\right\} + \frac{\partial c_g}{\partial x} = J(x)\, H(t-x). \tag{3.9}$$

This equation is solved numerically, again using the flux-limiter of Van Leer. The results are shown in Figure 8 where we used a Langmuir isotherm for adsorption given by

$$\phi(c_g) = \frac{3c_g}{1+c_g}. \tag{3.10}$$

The values of the coefficients in isotherm (3.10) are unrealistic. They were chosen to illustrate the behaviour of the gel profile ahead of the shock. In Figure 8 we see the following four features:

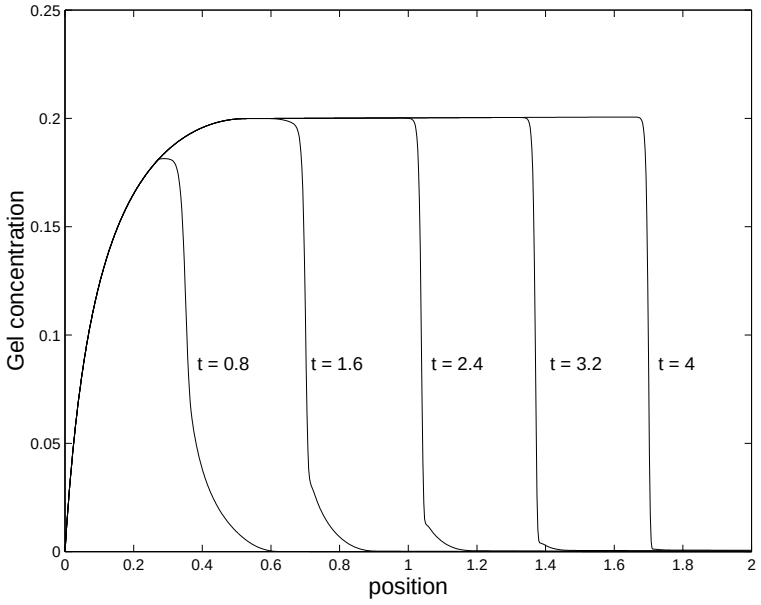

Figure 8: Gel concentration profiles, with $k_a = \infty$ and Φ given by 3.10, at times: $t = 0.8$, 1.6, 2.4, 3.2 and 2. Input data are taken from Table 1.

1. The occurrence of a shock, located at $x = s(t)$. Its speed, $\dot{s}(t)$, is given by the Rankine-Hugoniot condition

$$\dot{s}(t) = \frac{c_g(s_-(t),t) - c_g(s_+(t),t)}{c_g(s_-(t),t) + A(s_-(t),t) - c_g(s_+(t),t) - A(s_+(t),t)} < 1,$$

due to adsorption. Hence $s(t) < t$.

2. $c_g(x,t) = \overline{c}_g(x)$ for $0 < x < s(t)$, except near the shock due to numerical dispersion. This is explained by the method of characteristics. Along each characteristic, starting at the positive t-axis in the x,t plane, we have

$$\left.\begin{aligned} &\frac{dc_g}{dx} = J(x), \quad 0 < x < t, \\ &\frac{dt}{dx} = 1 + \phi'(c_g), \\ &c_g(0) = 0. \end{aligned}\right\} \qquad (19')$$

It is clear from characteristics emerging from the t-axis ($x = 0$) that as long as they do not intersect with characteristics emerging from the x-axis, the solution is independent of t. This results in the enveloping behaviour as observed in Figure 8. The characteristics of (19′) are illustrated in Figure 9. Due to the concave shape of $\phi(c_g)$, characteristics in the x,t-plane are concave as well.

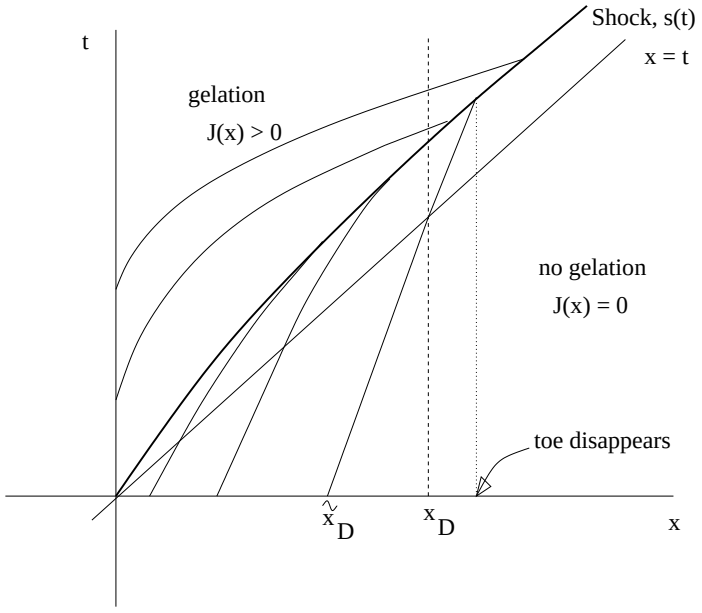

Figure 9: Sketch of characteristics of (19′), corresponding to Figure 8.

3. Occurence of a toe in the gel profiles for $s(t) < x < t$. This can be seen as follows. Each characteristic starting from the x-axis is at first a straight line, due to the absence of the source term for $x > t$. Since $\phi'(0) > 0$, we have $\frac{dt}{dx} > 1$ and hence these characteristics intersect the line $x = t$. After this intersection the source term becomes positive and since $\phi(c_g)$ is concave, the characteristics continue as concave curves as well, see Figure 9. These characteristics intersect with the ones starting at the t-axis resulting in the shock at $x = s(t)$. The positive source term gives an accumulation and hence a toe occurs between the shock and the position $x = t$.

4. Disappearance of the toe. Characteristics starting from the x-axis that will arrive at $x = t$ for $x \geq x_D$, will continue as straight lines towards the shock curve. In particular, the characteristics starting from $\tilde{x}_D = \frac{\phi'(0)}{1+\phi'(0)} x_D$, is the first one to satisfy this behaviour, see Figure 9. Consequently, the toe disappears at the intersection of this characteristic at the shock curve. Moreover, the shock proceeds with constant speed given by:

$$\dot{s}(t) = \frac{c_g^*}{c_g^* + \phi(c_g^*)},$$

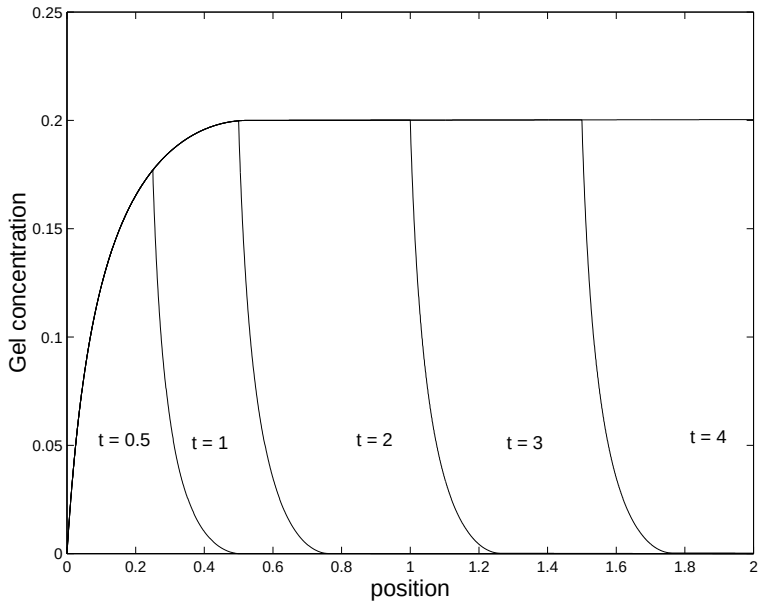

Figure 10: Gel profiles for times $t = 0.5$, 1, 2, 3 and $t = 4$. The adsorption isotherm is linear with $\alpha = 1$. Other input data are taken from Table 1.

When the adsorption isotherm is linear, i.e. $\phi(c_g) = \alpha\, c_g$, problem (19') can be solved explicitly in terms of $J(x)$. The corresponding gel profile is then given by

$$c_g(x,t) = \begin{cases} \int_0^x J(s)ds, & 0 \le x \le \frac{t}{1+\alpha}, \\ \int_{\frac{(1+\alpha)x-t}{\alpha}}^x J(s)ds, & \frac{t}{1+\alpha} < x \le t, \\ 0, & x > t. \end{cases}$$

Since characteristics do not intersect in this case (i.e. $\dfrac{dt}{dx} = 1 + \alpha$) no shock occurs at the toe for all $x > 0$, see Figure 10.

For finite adsorption rate we find smooth gel profiles. This is shown in Figures 11 and 12. In Figure 11 we used $k_a = 1$ to illustrate the gradual build-up of the adsorbed concentration. In Figure 12 we used the larger value $k_a = 10$, to illustrate the travelling wave behaviour at the leading edge of the profile for large values of t. As intermediate constant state we find again $c_g = c_g^*$ and $A = A(c_g^*)$. Following van Duijn & Knabner [6] we can determine the shape at speed of this wave by considering the following problem, for $-\infty < x < \infty$,

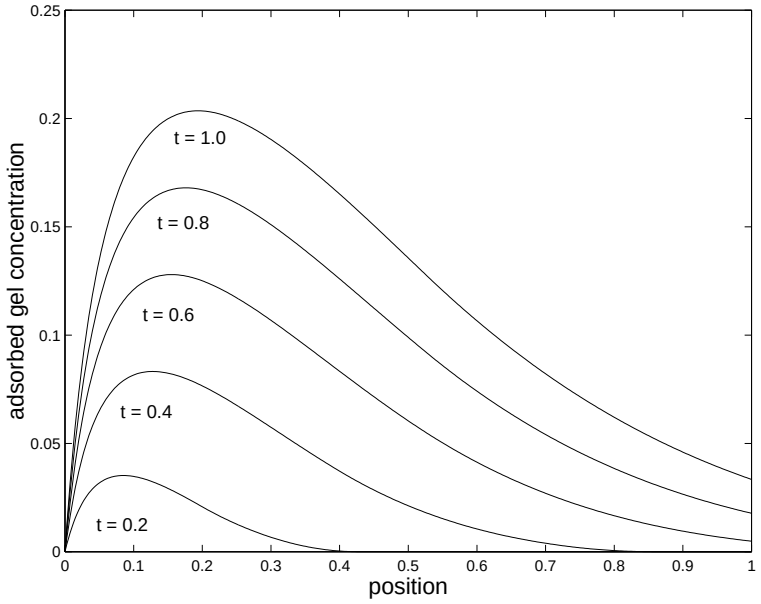

Figure 11: Adsorbed gel profiles for times $t = 0.2, 0.4, 0.6, 0.8$ and $t = 1$. The adsorption isotherm is taken from Langmuir, see equation 3.10. The adsorption rate constant is $k_a = 1$. All other data are taken from Table 1.

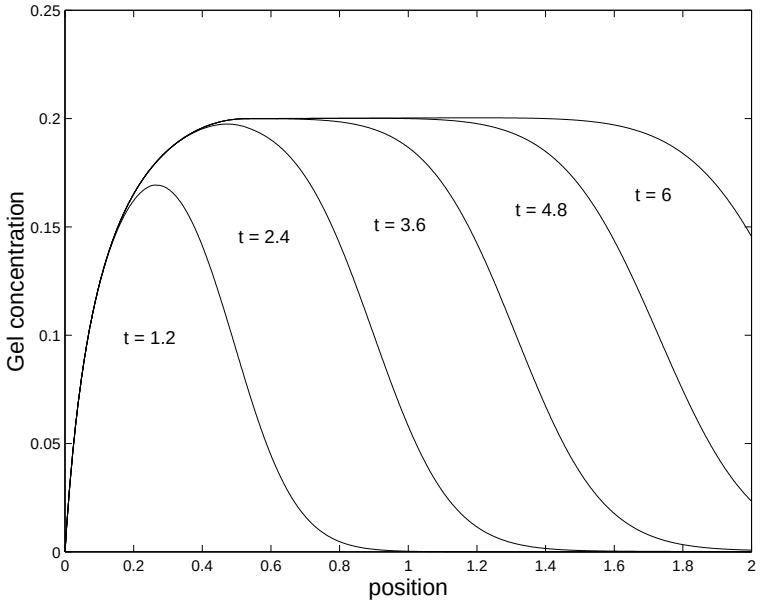

Figure 12: Gel profiles for times $t = 1.2, 2.4, 3.6, 4.8$ and $t = 6$. The adsorption isotherm is taken from Langmuir, see equation 3.10. The adsorption rate constant is $k_a = 10$. All other data are taken from Table 1.

$t > 0$:

$$\begin{cases} \dfrac{\partial c_g}{\partial t} + \dfrac{\partial A}{\partial t} + \dfrac{\partial c_g}{\partial x} = 0 \\ \dfrac{\partial A}{\partial t} = k_a(\phi(c_g) - A) \\ c_g(-\infty, t) = c_g^* \qquad\qquad A(-\infty, t) = \phi(c_g^*) \\ c_g(\infty, t) = 0 \qquad\qquad A(\infty, t) = 0 \end{cases}$$

Setting $\eta = x - st$ and considering solutions of the form $c_g = c_g(\eta)$, $A = A(\eta)$, we arrive at, for $-\infty < \eta < \infty$

$$\begin{cases} -s\,(c_g' + A') + c_g' = 0 \\ -sA' = k_a(\phi(c_g) - A) \\ c_g(-\infty) = c_g^* \qquad\qquad A(-\infty) = \phi(c_g^*) \\ c_g(\infty) = 0 \qquad\qquad A(\infty) = 0. \end{cases}$$

The boundary conditions directly imply

$$s = \frac{c_g^*}{c_g^* + \phi(c_g^*)},$$

which is in close agreement with the results obtained in Figure 12. The boundary conditions at $\eta = +\infty$ also imply

$$c_g = \frac{s}{1-s} A,$$

which leaves us with the integral equation

$$\int_{c_g(\eta_1)}^{c_g(\eta)} \frac{d\sigma}{\phi(\sigma) - \frac{s}{1-s}\sigma} = \frac{k_a}{s-1}(\eta - \eta_1),$$

from which the leading edge profiles for c_g and A can be determined. To match the location of the wave with the leading edge front an additional argument is needed. We locate the wave in the x, t plane so that its center of mass co-incides with the location of the shock when $k_a = \infty$ (see Figure 9, for x and t sufficiently large). This amounts to the following. First determine η_1 so that $x - st - \eta_1$ matches the shock curve in Figure 9 once it becomes linear. The corresponding value $c_g(\eta_1)$ is now selected so that the shaded regions in Figure 13 have equal area.

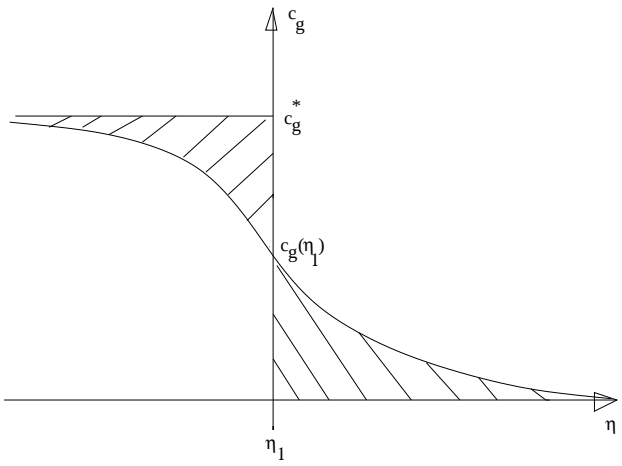

Figure 13: Travelling wave profile with $c_g(\eta_1)$ selected so that $\int_{-\infty}^{\eta_1}(c_g^* - c_g(s))ds = \int_{\eta_1}^{\infty} c_g(s)ds$.

4. Conclusions

In this paper we developed a model for the transport of polymers, crosslinkers, gel in combination with chemical reactions. This model predicts the following:

- Concentration profiles do not depend on initial acidity in the reservoir when dispersion is absent.
- Crosslinker precipitation is consequently also independent on initial acidity.
- When crosslinker precipitation takes place, then precipitated crosslinker increases linearly with time.
- Gelation reaction results in a pulse-like gel-profile and develops in a constant state preceeded by a travelling wave with a constant speed.

Acknowledgement This work was funded by the European Union (Welgel project) and by the Welgel industrial consortium (BGplc, GDF, Halliburton, Norsk-Conoco, Petrobas, Shell, SNF-Floerger, Statoil, Tarim Oilfield, Texaco and Total). Dr. Joost Hulshof and Dr. Pacelli Zitha are acknowledged for a number of fruitful discussions.

References

1. Rainer Helmig. *Multiphase flow and transport processes in the subsurface.* 1. Springer, Stuttgart, July 1997.
2. W.H. Hundsdorfer, B. Koren, M. van Loon, and J.G. Verwer. A positive finite-difference advection scheme. *Journal of Computational Physics*, 117, 1995.
3. P. Knabner, C.J. van Duijn, and S. Hengst. An analysis of crystal dissolution fronts in flows through porous media. part 1: Compatible boundary conditions. *Advances in water resources*, 18,3:171–185, 1995.
4. Randall J. LeVeque. *Numerical methods for conservation laws.* 2. Birkhäuser Verlag, Zürich, 1992.
5. L. Surguchev and A. Stavland. Water shut-off: simulation and laboratory evaluation. *Proceedings of the* 60^{th} *EAGE conference*, Leipzig, 1998.
6. C.J. van Duijn and P. Knabner. Flow and reactive transport in porous media induced by well injection: similarity solution. *IMA J. of Applied Mathematics*, 52, 1994.
7. B. van Leer. Towards the ultimate conservative difference scheme. iii. upstream-centered finite-difference schemes for ideal compressible flow. *Journal of Computational Physics*, 23:276–299, 1977.
8. P.L.J. Zitha and C.W. Botermans. Bridging adsorption of flexible polymers in low-permeability porous media. *SPE Society of Petroleum Engineers (Production and Facilities)*, Februari 1998, 1998.
9. P.L.J. Zitha, F.J. Vermolen, and J. Bruining. Modification of two-phase flow properties by adsorbed polymers and gels. *SPE Society of Petroleum Engineers*, SPE 54737, 1999.